SCIENCE CHINA
Technological Sciences

October 2011 Vol.54 No.10: 2618–2628
doi: 10.1007/s11431-011-4510-1

Numerical simulation of deposit in confluence zone of debris flow and mainstream

CHEN RiDong, LIU XingNian, CAO ShuYou & GUO ZhiXue*

State Key Laboratory of Hydraulics and Mountain River Engineering, Sichuan University, Chengdu 610065, China

Received November 16, 2010; accepted May 3, 2011; published online August 25, 2011

Abundant solid materials were formed as a result of landslide and collapse due to Wenchuan earthquake. The solid source around mountains would form a debris flow when appropriate rain condition occurs. Such a debris flow is structurally very large and strong, and the river flow can hardly wash away the deposit when the debris flow enters into the mainstream. As a result, the deposit on the river bed due to debris flow will cause a series of hazards. Based on the previous researches and relevant data, this paper simplified the interaction between debris flow and current of the main river, and adopted the finite element characteristic-based-split algorithm which is favorable to the stabilization of dealing with the convection. Finally, the numerical model of the confluence of debris flow deposit and main river was developed, and the deposit progress of the mega-debris flow from Wenjiagou in Mianyuan river was reproduced. Furthermore, the influence of the deposit on the flow route of the main river, and distribution of velocity and water depth were analyzed. The results showed that the simulation deposit terrain qualitatively agreed with the field data through comparison, including the deposit area and depth distribution. Furthermore, the improvement of the model in future was discussed.

torrential flood, debris flow, confluence zone, FEM

Citation: Chen R D, Liu X N, Cao S Y, et al. Numerical simulation of deposit in confluence zone of debris flow and mainstream. Sci China Tech Sci, 2011, 54: 2618–2628, doi: 10.1007/s11431-011-4510-1

1 Introduction

It is well-known that debris flows contain a large amount of solid particles (especially the particles of large size). When the debris flows enter a main river laterally, it will cause intensive interaction between water and sediment. Dramatic change of the river bed morphology in the region of the confluence will occur not only due to changes of the topographic condition maintaining the movement of the debris flow, but also due to the resistance of the main river. Generally, the terrain of the confluence of two rivers is relatively mild, where it is an important place of human living and activities, and it becomes a major area often associated with catastrophic disaster caused by debris flow depositing. For example, the large-scale glacial debris flows occurred in Peilong Valley nearby Sichuan-Tibet highway in Tibet successively in 1984 and 1985, and they blocked the main stream of Purlung Tsangpo River and formed a 6.5 km long barrier lake with a maximum width and depth being 220 and 14.3 m, respectively, whose backwater flooded nearly 7.0 km highway; hence many people were killed and economic losses were over 100 million yuan [1]. As a result, the Bolo power plant, located at the confluence between Wahei River and Xianjiapu River in Mabian Yi autonomous county Sichuan province, was flooded only one year after its completion. After the disaster, the elevation of the flood defense wall was increased further by 1.05–3.16 m. However just 10 months later, in 2001 July 28, due to heavy rain a debris

*Corresponding author (email: scugzx@scu.edu.cn)

flow caused huge debris flow deposit in the confluence, which led to catastrophic damage to the plant. The sedimentation thickness within the river reach of the plant was about 5.0–7.5 m, the plant was submerged completely with an average 7.5 m thick sedimentation inside the plant [2]. After Wenchuan earthquake, increasing loose debris triggered by rainfall enhances the chance of outbreak of debris flows. In 2010, debris flows occurred in the earthquake disaster region of Wenchuan, such as Yingxiu (Hongchungou), Qingping (Wenjiagou), etc., entered the main river channel, and generated large deposition and caused disasters. Therefore, it is most important to investigate the feathers of confluence deposition of debris flow in the main river.

When debris flows enter into a main river, it involves complex interaction between non-Newtonian fluids and Newton fluids. There are several difficulties in theoretical studies [3]. Meanwhile, due to the technical limitation of observation method, it is difficult to obtain the confluence data under both field and laboratory conditions and to find a relationship between flume experiment and natural situation. The prototype observation or experimental study is not only costly but also difficult to carry out [4]. Therefore, numerical simulation is an alternative research method used by many researchers.

At present, the majority of research is undertaken on the water flow movement in the confluence of debris flow and main river, both theoretically and numerically, particularly the latter has shown some relatively good results. So is for silt-laden water flow movement [5, 6], which has shown to meet the requirement of practical engineering [7, 8]. For numerical modeling on a single debris flow, Wang [9] proposed a flow regiment model of debris flow based on two-phase flow theory and established the corresponding equations and numerical solutions. Flow regiment model is a simple model with good numerical stability, especially suitable for large-scale flow. Hübl et al. [10] simulated the deposition processing of two viscous debris flows by combining the secondary rheological model with DEM, where the simulation process included topography, geology, hydrology, etc. Iovine et al. [11] modeled the debris flows with strong inertial effects using a hexagonal S_{4a} cellular automata model calibrated by genetic algorithms. Diego Berzi et al. [12] summarized the latest development of debris flow particles-fluid model and its application to theoretical explanation of the complex constitutive relation of debris flow. It is clear that much progress of numerical modeling has been made in practical application, interdisciplinary integration, improvement of algorithm, and theoretical studies of debris flow. However, a large number of works and case studies [13] have shown that some unsolved difficulties exist in the studies of debris flow dynamics, such as incompleteness and adoptability of the existing constitutive model of debris flow dynamics, model selection due to disagreement on the available numerical simulation methods, far more difficulties about complex environmental effect of debris flow dynamics, under-development of coupling algorithm of debris flow dynamics numerical model, etc. All these aspects have significant influences on the accuracy and practicality of numerical modeling on debris flow dynamics. Therefore, any existing numerical model of debris flow has to some degree limitation in practical applications.

Compared with the research on single flow aspect, the research progress of confluence numerical model is relatively slow. At present, the study on governing equations to fully describe the debris flow entering into the main river is still in the early stage. There is little investigation on discussion or simulation of deposition process of debris flow, particularly on an actual deposition process of debris flow. It is difficult to establish a mathematical deposition model of debris flow confluence with river. The main reasons are: the difficulties associated with the numerical model of debris flow, and the different approaches used by the researchers. Due to the complex mechanism of debris flow confluence with the main river, it is difficult and unachievable that the debris flow and river flow are solved as a simple system. However, it is much simple and feasible to simulate the movements of debris flow and water flow independently and then complete the calculation of confluence by taking account of the interaction between the two. However, two issues arise in such a method. First, when only the debris flow is simulated, what model among so many existing debris flow models is selected for use in order to meet the requirement of practical application? Second, how to express the interaction mechanism between debris flow and river flow? In a word, the confluence of debris flow and river flow is a complex problem with interaction between non-Newtonian fluid and Newton fluid, as both of them are difficult to quantify on the interface, therefore the researchers have to make simplification or assumption to propose interaction mechanism. Third, the algorithm is selected for the simulation of both water flow and debris flow for the convenience of storage and calculation. As the river bed topography of the confluence area changes dramatically, it requires good stabilization of the algorithm. Therefore, the researchers have to consider the generality and stabilization of the algorithm. In view of the above factors, based on the debris flow regiment model [14], appropriate simplification on the interaction between debris flow and main stream water flow at the confluence area, this paper presents a finite element method with a characteristic-based-split algorithm to handle the convection term, and proposes a mathematical model of deposition of debris flow confluence with main river. By using the model, fluid confluence deposition processes with two different constitutive relations between the mainstream and tributary are simulated and compared with the field data.

2 Numerical model

2.1 Control equations of model

A large number of field measurements show that debris flow has features of the two phase flow. For a general debris flow, a critical grain size always exists in the body comprised of water and a wide range of size of solid particles, which makes fine particles less than the critical grain size form a non-separated slurry with water, and coarse particles, larger than the critical grain size, move less than the slurry flow. It is called the sorting phenomenon. However, when debris flow has high concentration and large velocity, the internal force of debris flow distributes in a slurry and such a sorting phenomenon is not obvious. Therefore, the debris flow model proposed ref. [14] is used, that is, a single flow model in combination with the concept of two phase flow structure to model the resistance item for debris flows. The governing equations of two-dimensional viscous debris flow are described as

$$\frac{\partial h}{\partial t}+\frac{\partial hu}{\partial x}+\frac{\partial hv}{\partial y}=0, \tag{1}$$

$$\begin{aligned}\frac{\partial hu}{\partial t}+\frac{\partial hu^2}{\partial x}+\frac{\partial huv}{\partial y}&=-gh\frac{\partial(z_o+h)}{\partial x}\\&-gh\left(\frac{\tau_B}{\gamma_m h}\operatorname{sgn}(u)+\frac{2\mu_B u}{\gamma_m h^2}+\eta_B\operatorname{sgn}(u)\right)\\&+\frac{\mu_m gh}{\gamma_m}\left(\frac{\partial^2 u}{\partial x^2}+\frac{\partial^2 u}{\partial y^2}\right),\end{aligned} \tag{2}$$

$$\begin{aligned}\frac{\partial hv}{\partial t}+\frac{\partial huv}{\partial x}+\frac{\partial hv^2}{\partial y}&=-gh\frac{\partial(z_o+h)}{\partial y}\\&-gh\left(\frac{\tau_B}{\gamma_m h}\operatorname{sgn}(v)+\frac{2\mu_B v}{\gamma_m h^2}+\eta_B\operatorname{sgn}(v)\right)\\&+\frac{\mu_m gh}{\gamma_m}\left(\frac{\partial^2 v}{\partial x^2}+\frac{\partial^2 v}{\partial y^2}\right).\end{aligned} \tag{3}$$

The right terms of eqs. (2) and (3) are the slope of gravity, the boundary resistance (including liquid Bingham body stress, viscous force, and friction of solid phase), and acceleration generated by interaction among flow regiments, respectively. In eqs. (1)–(3), h is depth, u and v are velocities of debris flow, g is the acceleration of gravity, z_o is the elevation of original terrain, τ_B, γ_m, μ_B and η_B mean the elevation of original terrain, Bingham stress of slurry, volumetric weight of debris flow, and the viscosity coefficient of slurry, respectively. The friction gradients of solid phase $\operatorname{sgn}(u)=\pm1$ and $\operatorname{sgn}(v)=\pm1$ show the signs of 2-D velocity vector in x and y directions, respectively. The liquid-solid critical grain sizes of debris flow and relevant characteristic parameters are determined according to the values in ref. [14].

The governing equations of 2-D shallow water flow are

$$\frac{\partial \eta}{\partial t}+\frac{\partial DU}{\partial x}+\frac{\partial DV}{\partial y}=0, \tag{4}$$

$$\begin{aligned}\frac{\partial UD}{\partial t}+\frac{\partial U^2 D}{\partial x}+\frac{\partial UVD}{\partial y}&=-gD\frac{\partial D}{\partial x}+gDi_x\\&-\frac{n^2 g\sqrt{U^2+V^2}}{D^{1/3}}U+\frac{\partial}{\partial x}\left(D\tau_{xx}\right)+\frac{\partial}{\partial y}\left(D\tau_{xy}\right),\end{aligned} \tag{5}$$

$$\begin{aligned}\frac{\partial VD}{\partial t}+\frac{\partial UVD}{\partial x}+\frac{\partial V^2 D}{\partial y}&=-gD\frac{\partial D}{\partial y}+gDi_y\\&-\frac{n^2 g\sqrt{U^2+V^2}}{D^{1/3}}V+\frac{\partial}{\partial x}\left(D\tau_{xy}\right)+\frac{\partial}{\partial y}\left(D\tau_{yy}\right),\end{aligned} \tag{6}$$

where η is water level, D is water depth, U and V are flow velocities, i_x and i_y are slopes of terrain, n is roughness coefficient of river bed, $\tau_{xx}=2\nu_t\frac{\partial U}{\partial x}$, $\tau_{xy}=\tau_{yx}=\nu_t\left(\frac{\partial U}{\partial y}+\frac{\partial V}{\partial x}\right)$, $\tau_{yy}=2\nu_t\frac{\partial V}{\partial y}$, ν_t is horizontal viscosity coefficient of turbulence, which is solved by Smagorinsky vortex viscous model:

$$\nu_t=0.12A\left[\left(\frac{\partial U}{\partial x}\right)^2+0.5\left(\frac{\partial V}{\partial x}+\frac{\partial U}{\partial y}\right)^2+\left(\frac{\partial V}{\partial y}\right)^2\right]^{0.5},$$

where A is the area of region influenced by nodes.

The governing equations of sediment transport in flow are

$$(1-\xi)\frac{\partial z_b}{\partial t}+\frac{\partial q_{bx}}{\partial x}+\frac{\partial q_{by}}{\partial y}=\frac{\alpha\omega}{\rho_s}\left(S-S^*\right), \tag{7}$$

$$\begin{aligned}\frac{\partial DS}{\partial t}+\frac{\partial UDS}{\partial x}+\frac{\partial VDS}{\partial y}&=\frac{\partial}{\partial x}\left(D\nu_t\frac{\partial S}{\partial x}\right)\\&+\frac{\partial}{\partial y}\left(D\nu_t\frac{\partial S}{\partial y}\right)+\alpha\omega\left(S^*-S\right),\end{aligned} \tag{8}$$

where ω is the settling velocity of sediment, z_b is the thickness of moving layer, ξ is the porosity of moving layer, α is the coefficient of imbalances sediment transport, S is sediment concentration of suspended load, S^* is the sediment-carrying capacity of suspended load, and q_{bx} and q_{by} are the sediment transport rates of bed load.

If the influence of debris flow on sediment transport on river bed is taken into account, similar to the calculation of bed load sediment transport rate of flow, the sediment continuous equation of debris flow is as follows:

$$(1-\xi)\frac{\partial z_b}{\partial t}+\frac{\partial q_{bx}}{\partial x}+\frac{\partial q_{by}}{\partial y}=0. \quad (9)$$

In this paper Mayer-Peter formulae of the bedload transport rate are used:

$$q_{bx}=8\sqrt{\left(G-\frac{\rho}{\rho_W}\right)gd^3}\,\frac{U}{\sqrt{U^2+V^2}}\max\left(\tau_*-\tau_{*,c},0\right)^{1.5},$$

$$q_{by}=8\sqrt{\left(G-\frac{\rho}{\rho_W}\right)gd^3}\,\frac{V}{\sqrt{U^2+V^2}}\max\left(\tau_*-\tau_{*,c},0\right)^{1.5},$$

where G is the relative density of sediment and water, d is a particle size for one grading. $\tau_*=\dfrac{n^2\left(U^2+V^2\right)^{1.5}}{\left(G-\rho/\rho_W\right)dD^{1/3}}$ is the shear stress, and $\tau_{*,c}=0.047$ is critical shear stress. For flow, ρ, U and V are water density and water flow velocities, respectively; for debris flow, ρ, U and V are the density and velocities of debris flow, respectively. The formula of sediment-carrying capacity is $S^*=k\left(\dfrac{\left(U^2+V^2\right)^{1.5}}{gD\omega}\right)^m$, where the empirical constants k=0.07, m=1.14 and α=0.3 are used. The separated particle size between bed load and suspended load is determined by a suspension index: $Rz=\dfrac{\omega}{cu_*}$, where c is Kaman constant, and u_* is bed shear velocity. It follows that Rz=4.166 according to the bursting theory [15], that is, Rz>4.166 for bed load for and $Rz\leqslant$4.166 for suspended load.

2.2 Simplification and solution of model

Due to the complex mechanism of debris flow confluence with the river flow, if the debris flow and river flow are solved as a whole, it will be very difficult and unrealistic. Therefore, in this paper the method is that both debris flow and the flow of mainstream are simulated separately and then compute the confluence through the function relation between debris flow and river flow. The interaction mechanism between them is simplified as follows: The prime influence of debris flow on water flow is changes of topography, and the other influences are secondary [16]; whereas only the changes of mud depth caused by sediment transport are considered when water flow affects debris flow.

The solving process of the model is as follows: First, to compute the characteristic parameters after determination of the critical grain size based on the bulk of debris flow and the gradation; to estimate initial mud depth of debris flow according to the debris flow discharge and the empirical formula. The flow field of mainstream is obtained by iterations with the mainstream flow boundary condition of upstream discharge and downstream water level . Then in each time step: 1. Solving debris flow governing equations, and the corresponding sediment continuity equation, that is, solving the transport of debris flow and changes of topography caused by the deposition of debris flow based on the boundary conditions of debris flow. 2. Solving the shallow water equations and sediment transport equations, that is, solving the sediment transport in the mainstream, and the impacts on mud depth by sediment transport based on the boundary conditions of mainstream flow.

2.3 Numerical implementation

The finite element method is an important method solving the various complex mathematical physics problems. Galerkin process is optimal in solving the self-adjoint problem. However, convection plays a dominated role in most fluid mechanics problems, where the convection term needs special treatment to ensure the stabilization of the method, and then Galerkin process is no longer optimal for such phenomena. Therefore, Zienkiewicz and Codina [17] proposed the finite element characteristic-based-split algorithm (CBS). The format of CBS algorithm is simple and stable to handle the convection term. From the existing calculated results, this algorithm is applicable to all ranges of flow and gives at least similar results to those by other methods [18]. The requirement on stabilization of the method is needed in modeling debris flow or flow of the mountain rivers with steep slopes, where both flow discharge and riverbed have large variation. However, the application of CBS algorithm in debris flow or flow of the mountain rivers has not been reported. To improve the calculation efficiency and model stabilization, this paper uses CBS algorithm as an attempt. The details about the characteristic-Galerkin procedures and the split-temporal discretization and split-spatial discretization can be seen in ref. [18]. The following is an introduction of solution procedure of the model.

1) Solution procedure of debris flow.

For simplicity, let $\boldsymbol{R}=\begin{pmatrix}\boldsymbol{hu}\\ \boldsymbol{hv}\end{pmatrix}$, $\boldsymbol{r}=\begin{pmatrix}\boldsymbol{u}\\ \boldsymbol{v}\end{pmatrix}$ and $\boldsymbol{i}=\begin{pmatrix}\boldsymbol{i}_x\\ \boldsymbol{i}_y\end{pmatrix}$. $\boldsymbol{i}_x=-\dfrac{\partial\left(z_o+\boldsymbol{h}\right)}{\partial x}$ and $\boldsymbol{i}_y=-\dfrac{\partial\left(z_o+\boldsymbol{h}\right)}{\partial y}$ are surface gradients of debris flow, and the solution procedure of matrix $\boldsymbol{R}^{n+1}$ is as follows:

$$\boldsymbol{R}^k=\boldsymbol{R}^0-\boldsymbol{M}^{-1}\alpha^k\Delta t\left(\left(\boldsymbol{CR}+\boldsymbol{S}_m\boldsymbol{r}-\boldsymbol{f}\right)-\Delta t\left(\boldsymbol{S}_s\boldsymbol{R}+\boldsymbol{f}_s\right)\right)^{k-1}, \quad (10)$$

$$\boldsymbol{h}^k=\boldsymbol{h}^{k-1}+\boldsymbol{M}^{-1}\Delta t\left(\boldsymbol{H}\left(\left(1-\theta_1\right)\boldsymbol{R}^{k-1}+\theta_1\boldsymbol{R}^k\right)-\boldsymbol{f}_h\right), \quad (11)$$

where

$$k=(1,2,3,4),\quad (\alpha^1,\alpha^2,\alpha^3,\alpha^4)=\left(\frac{1}{4},\frac{1}{3},\frac{1}{2},1\right),$$

$$\boldsymbol{R}^0=\boldsymbol{R}^n,\quad \boldsymbol{R}^{n+1}=\boldsymbol{R}^4,\quad \boldsymbol{h}^0=\boldsymbol{h}^n,\quad \boldsymbol{h}^{n+1}=\boldsymbol{h}^4.$$

$$\boldsymbol{M}=\int_\Omega \boldsymbol{N}^{\mathrm{T}}\boldsymbol{N}\mathrm{d}\Omega,\quad \boldsymbol{C}=\int_\Omega \boldsymbol{N}^{\mathrm{T}}\left(\boldsymbol{\nabla}\left(\boldsymbol{rN}\right)\right)\mathrm{d}\Omega,$$

$$\boldsymbol{S}_m=\int_\Omega\left(\boldsymbol{\nabla N}\right)^{\mathrm{T}}\boldsymbol{\nabla N}\frac{\boldsymbol{\mu}_m g\boldsymbol{h}}{\gamma_m}\mathrm{d}\Omega,$$

$$\boldsymbol{S}_s=-\frac{1}{2}\int_\Omega\left(\boldsymbol{\nabla}^{\mathrm{T}}\left(\boldsymbol{rN}\right)\right)^{\mathrm{T}}\left(\boldsymbol{\nabla}^{\mathrm{T}}\left(\boldsymbol{rN}\right)\right)\mathrm{d}\Omega,$$

$$\boldsymbol{f}=\int_\Omega \boldsymbol{N}^{\mathrm{T}}\boldsymbol{N}g\left(\boldsymbol{hi}-\left(\frac{\boldsymbol{\tau}_B}{\gamma_m}+\boldsymbol{h\eta}_B\right)\mathrm{sgn}(\boldsymbol{r})-\frac{2\boldsymbol{\mu}_{\mathrm{B}}\boldsymbol{r}}{\gamma_m\boldsymbol{h}}\right)\mathrm{d}\Omega,$$

$$\boldsymbol{f}_s=-\frac{1}{2}\int_\Omega\left(\left(\boldsymbol{\nabla}^{\mathrm{T}}\left(\boldsymbol{rN}\right)\right)^{\mathrm{T}}\boldsymbol{N}g\left(\boldsymbol{hi}-\left(\frac{\tau_B}{\gamma_m}+\boldsymbol{h\eta}_B\right)\mathrm{sgn}(\boldsymbol{r})-\frac{2\mu_B\boldsymbol{r}}{\gamma_m\boldsymbol{h}}\right)\right)\mathrm{d}\Omega,$$

$$\boldsymbol{H}=\int_\Omega\left(\boldsymbol{\nabla N}\right)^{\mathrm{T}}\boldsymbol{N}\mathrm{d}\Omega,$$

$$\boldsymbol{f}_h=\int_\Gamma \boldsymbol{N}^{\mathrm{T}}\boldsymbol{e}^{\mathrm{T}}\left(\left(1-\theta_1\right)\boldsymbol{R}^{k-1}+\theta_1\boldsymbol{R}^k\right)\mathrm{d}\Gamma.$$

$\boldsymbol{N}$ is the shape function. $0.5\leqslant\theta_1\leqslant 1$ is the artificial compression parameter. $\boldsymbol{e}$ is the boundary normal unit vector.

2) The solution procedure of flow.

Let $\boldsymbol{R}=\begin{pmatrix}\boldsymbol{DU}\\ \boldsymbol{DV}\end{pmatrix}$, $\boldsymbol{r}=\begin{pmatrix}\boldsymbol{U}\\ \boldsymbol{V}\end{pmatrix}$ and $\boldsymbol{i}=\begin{pmatrix}\boldsymbol{i}_x\\ \boldsymbol{i}_y\end{pmatrix}$. $\boldsymbol{i}_x$ and $\boldsymbol{i}_y$ are the slopes of terrain, and the solution procedure of matrix $\boldsymbol{R}^{n+1}$ is as follows.

First step: solving the variation of velocity $\Delta\boldsymbol{R}^*$:

$$\begin{aligned}\Delta\boldsymbol{R}^*&=\boldsymbol{R}^*-\boldsymbol{R}^n\\&=-\boldsymbol{M}^{-1}\Delta t\left(\left(\boldsymbol{CR}+\boldsymbol{K}_m\boldsymbol{r}-\boldsymbol{f}\right)-\Delta t\left(\boldsymbol{K}_s\boldsymbol{R}+\boldsymbol{f}_s\right)\right)^n.\end{aligned}\quad(12)$$

Second step: solving the variation of depth $\Delta\boldsymbol{D}$:

$$\Delta\boldsymbol{D}=\boldsymbol{M}^{-1}\Delta t\left(\boldsymbol{H}\left(\boldsymbol{R}^n+\theta_1\Delta\boldsymbol{R}^*\right)-\Delta t\theta_1\boldsymbol{G}\boldsymbol{p}^n-\boldsymbol{f}_h\right).\quad(13)$$

Third step: using $\Delta\boldsymbol{D}$ and correcting $\Delta\boldsymbol{R}^*$ to get the value of t^{n+1}:

$$\boldsymbol{D}^{n+1}=\boldsymbol{D}^n+\Delta\boldsymbol{D},\quad(14)$$

$$\boldsymbol{R}^{n+1}=\boldsymbol{R}^n+\Delta\boldsymbol{R}^*-\boldsymbol{M}^{-1}\Delta t\left(\boldsymbol{H}^{\mathrm{T}}\left(\left(1-\theta_2\right)\boldsymbol{p}^n+\theta_2\boldsymbol{p}^{n+1}\right)\right),\quad(15)$$

where

$$\boldsymbol{M}=\int_\Omega \boldsymbol{N}^{\mathrm{T}}\boldsymbol{N}\mathrm{d}\Omega,\quad \boldsymbol{C}=\int_\Omega \boldsymbol{N}^{\mathrm{T}}\left(\boldsymbol{\nabla}\left(\boldsymbol{rN}\right)\right)\mathrm{d}\Omega,$$

$$\boldsymbol{K}_m=\int_\Omega\left(\boldsymbol{\nabla N}\right)^{\mathrm{T}}\boldsymbol{\nabla N}\boldsymbol{v}_t\boldsymbol{D}\mathrm{d}\Omega,$$

$$\boldsymbol{K}_s=-\frac{1}{2}\int_\Omega\left(\boldsymbol{\nabla}^{\mathrm{T}}\left(\boldsymbol{rN}\right)\right)^{\mathrm{T}}\left(\boldsymbol{\nabla}^{\mathrm{T}}\left(\boldsymbol{rN}\right)\right)\mathrm{d}\Omega,$$

$$\boldsymbol{H}=\int_\Omega\left(\boldsymbol{\nabla N}\right)^{\mathrm{T}}\boldsymbol{N}\mathrm{d}\Omega,$$

$$\boldsymbol{G}=\int_\Omega\left(\boldsymbol{\nabla N}\right)^{\mathrm{T}}\boldsymbol{\nabla N}\mathrm{d}\Omega,$$

$$\boldsymbol{f}=\int_\Omega \boldsymbol{N}^{\mathrm{T}}\boldsymbol{N}g\boldsymbol{D}\left(\boldsymbol{i}-\frac{n^2\boldsymbol{r}\sqrt{\boldsymbol{U}^2+\boldsymbol{V}^2}}{\boldsymbol{D}^{4/3}}\right)\mathrm{d}\Omega,$$

$$\boldsymbol{f}_s=-\frac{1}{2}\int_\Omega\left(\left(\boldsymbol{\nabla}^T\left(\boldsymbol{rN}\right)\right)^{\mathrm{T}}\boldsymbol{N}g\boldsymbol{D}\left(\boldsymbol{i}-\frac{n^2\boldsymbol{r}\sqrt{\boldsymbol{U}^2+\boldsymbol{V}^2}}{\boldsymbol{D}^{4/3}}\right)\right)\mathrm{d}\Omega,$$

$$\boldsymbol{f}_h=\int_\Gamma \boldsymbol{N}^{\mathrm{T}}\boldsymbol{e}^{\mathrm{T}}\left(\boldsymbol{R}^n+\theta_1\Delta\boldsymbol{R}^*\right)\mathrm{d}\Gamma,$$

$\boldsymbol{p}=\dfrac{g\boldsymbol{D}^2}{2}$. $0\leqslant\theta_2\leqslant 1$ is an explicit or implicit parameter. $\boldsymbol{e}$ is the boundary normal unit vector.

3) The solution procedure of sediment transport.

Let $\boldsymbol{r}=\begin{pmatrix}\boldsymbol{U}\\ \boldsymbol{V}\end{pmatrix}$ and $\boldsymbol{q}_b=\begin{pmatrix}\boldsymbol{q}_{bx}\\ \boldsymbol{q}_{by}\end{pmatrix}$. Solve the convection-diffusion equation of suspended load and the sediment continuity equation in water flow:

$$\begin{aligned}\boldsymbol{S}^{n+1}=&\boldsymbol{S}^n-\boldsymbol{M}^{-1}\Delta t\left(\boldsymbol{CS}+\boldsymbol{K}_m\boldsymbol{S}-\boldsymbol{f}\right)^n\\&+\boldsymbol{M}^{-1}\left(\Delta t\right)^2\left(\boldsymbol{K}_s\boldsymbol{S}+\boldsymbol{f}_s\right)^n,\end{aligned}\quad(16)$$

$$\boldsymbol{z}_b^{n+1}=\boldsymbol{z}_b^n-\frac{1}{1-\xi}\left(\boldsymbol{Hq}_b+\boldsymbol{f}_c\right).\quad(17)$$

Solve the sediment transport of debris flow:

$$\boldsymbol{z}_b^{n+1}=\boldsymbol{z}_b^n-\frac{1}{1-\xi}\boldsymbol{Hq}_b,\quad(18)$$

where

$$\boldsymbol{M}=\int_\Omega \boldsymbol{N}^{\mathrm{T}}\boldsymbol{N}\mathrm{d}\Omega,\quad \boldsymbol{C}=\int_\Omega \boldsymbol{N}^{\mathrm{T}}\left(\boldsymbol{\nabla}\left(\boldsymbol{rN}\right)\right)\mathrm{d}\Omega,$$

$$\boldsymbol{K}_m=\int_\Omega\left(\boldsymbol{\nabla N}\right)^{\mathrm{T}}\boldsymbol{\nabla N}\boldsymbol{v}_t\boldsymbol{D}\mathrm{d}\Omega,$$

$$\boldsymbol{K}_s=-\frac{1}{2}\int_\Omega\left(\boldsymbol{\nabla}^{\mathrm{T}}\left(\boldsymbol{rN}\right)\right)^{\mathrm{T}}\left(\boldsymbol{\nabla N}\right)\mathrm{d}\Omega,$$

$$\boldsymbol{f}=\int_\Omega \boldsymbol{N}^{\mathrm{T}}\boldsymbol{N}\alpha\boldsymbol{\omega}\left(\boldsymbol{S}^*-\boldsymbol{S}\right)\mathrm{d}\Omega,$$

$$\boldsymbol{f}_s=-\frac{1}{2}\int_\Omega\left(\boldsymbol{\nabla}^{\mathrm{T}}\left(\boldsymbol{rN}\right)\right)^{\mathrm{T}}\boldsymbol{N}\alpha\boldsymbol{\omega}\left(\boldsymbol{S}^*-\boldsymbol{S}\right)\mathrm{d}\Omega,$$

$$\boldsymbol{f}_c=\int_\Omega \boldsymbol{N}^{\mathrm{T}}\boldsymbol{N}\frac{\alpha\boldsymbol{\omega}}{\rho_s}\left(\boldsymbol{S}^*-\boldsymbol{S}\right)\mathrm{d}\Omega,$$

$$\boldsymbol{H}=\int_\Omega \boldsymbol{N}^{\mathrm{T}}\left(\boldsymbol{\nabla}^{\mathrm{T}}\boldsymbol{N}\right)\mathrm{d}\Omega.$$

In eqs. (10)–(18),

$\Delta t \leqslant \min\left(\frac{\boldsymbol{h}_{em}}{\sqrt{\boldsymbol{u}^2+\boldsymbol{v}^2}}, \frac{\boldsymbol{h}_{em}}{\boldsymbol{o}+\sqrt{\boldsymbol{U}^2+\boldsymbol{V}^2}}\right)$ is a time step, $\boldsymbol{h}_{em}$ is an element size, and $\boldsymbol{o}=\sqrt{g\boldsymbol{D}}$ is the velocity of shallow water wave.

2.4 Boundary conditions for the model

1) Inlet boundary: The inlet flow boundary is the actual hydrograph, and sediment boundary conditions are sediment concentrations under different gradations.

2) Outlet boundary: When the water flow of the outlet boundary is impacted by the downstream water flow, the first type of boundary conditions will be given, i.e., the outlet boundary condition of water flow is the actual stage hydrograph. Otherwise, the second type of boundary conditions will be given, i.e., the gradient of water depth at the water flow outlet is zero. Similarly, when the sediment transport of outlet boundary is impacted by the downstream riverbed, the actual riverbed elevation hydrograph shall be given, otherwise the gradient of riverbed elevation will be taken as zero.

3) Land boundary: Slip boundary condition is used.

4) Moving boundary: It refers to the boundary line of the computational domain. Dry and wet nodes and grids shall be marked in the model of this paper. The specific ideas are as follows: For determination of a dry or wet node, a node will be marked as a dry node when its water/mud depth is less than the minimum water/mud depth, otherwise it will be marked as a wet node. Furthermore, a grid including any dry node will be taken as a dry grid, as shown in Figure 1. When only one grid is wet among the impact grids of certain wet node, the node will be taken as a dry node. Both will not join in the calculation of current step. Thus, a smooth boundary line between dry and wet units will be obtained, as shown in Figure 2. The calculation of the current step will be completed using the slip boundary condition of the boundary line. It shall be determined before the next step of calculation whether the average value of the node elevation of the dry grid (two wet nodes) on the boundary line is greater than that of the grid elevations. If so, all nodes of the dry grid will be marked as wet nodes and the determination of dry or wet nodes in the current step is completed. After repeating all the above, the next step of calculation can be done.

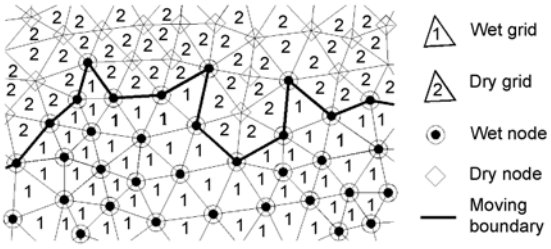

Figure 1 Unsmooth moving boundary.

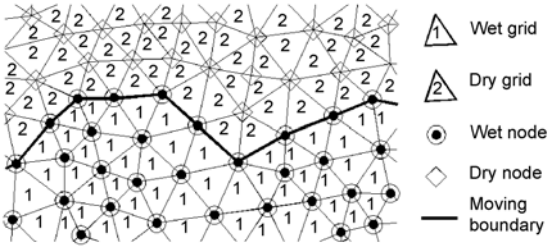

Figure 2 Smooth moving boundary.

3 Application of models

3.1 Overview of Wenjiagou debris flow

From the midnight of August 12, 2010 to the early morning of August 13, 2010, extraordinary rainstorm hit the area of Qingping township, Sichuan. And as a result super large-scale torrential floods and debris flows happened in five landslide gullies caused by Wenchuan earthquake along the Mianyuan River. The impact range was about 3 km long, 200–600 m wide and 2–18 m deep and about 7 million cubic meters materials deposited in the Mianyuan River. Of all the debris flows, the Wenjiagou debris flow was the largest, with an average flow discharge about 300 m^3/s and a duration of 5 h. And due to this debris flow, about 4.5 million cubic meters materials deposited at the gully mouth.

3.2 Parameters of the model

This paper reproduced the deposition process of the Wenjiagou debris flow considering the convergence with the mainstream through numerical models. Relevant characteristic parameters were determined by the method in ref. [14]. The debris flow discharge of the gully was given, the initial mud depth was obtained by the assumption of the debris flow velocity (the initial mud depth at the debris flow inlet was determined based on the assumption of 5 m/s initial velocity of the debris flow) and the actual mud depth was determined by the numerical model iterative calculation. The flow discharge at the mainstream inlet was 300 m^3/s and the sediment transport was saturated. Because the bridge deck of Xingfu Bridge built near Wenjiagou (which was rebuilt in 2009 after the Wenchuan earthquake) was washed downstream to the Old Qingping Bridge by the debris flow and stopped by the pier to block the bridge opening. As a result unsmooth water flow of the Mianyuan River was formed, and the water level at the site of Qingping Bridge was elevated to the deck, so the downstream water level in the model was approximately taken as the elevation of Qingping Bridge deck, i.e. 874.5 m. Results from the field survey indicated a wide graduation of Wenjiagou debris flow. Considering the calculation efficiency, the sediment graduation for calculation was divided into 12 levels

and the movable layer of each level was set with a thickness of 1 m and a porosity of 0.2. And the calculation method for non-uniform sediment is the bed-sediment-grouping method. In order to correct the defect of omission of the interaction between coarse and fine grains in such a method, an exposure degree coefficient [19] was used to reflect the interaction of sediment carrying capacities between various levels of sediments. The critical water depth of the dry/wet nodes was assumed as 0.05 m, and the critical mud depth 0.1 m. And the roughness coefficient was set as 0.045. In order to adapt to the dramatic variation of mud depth in some deposition zone, h-refinement process adaptive refined mesh [18] was applied. And the time step referred to adaptive time step [20]. Figure 3 shows the last adaptive refined grid.

3.3 Analysis on calculation results

The debris flow deposition thickness isograms (Figures 4, 5 and 6) show that the debris flow firstly deposits at the gully mouth and distributes little at the opposite bank and the downstream confluence mouth as well. And with the completion of debris flow bedding, the deposits gradually grow thick on the alluvial fan as the debris flow distributes to and expands towards the opposite bank and the downstream, particularly in the gully outlet area where the regional change is significant. The debris flow mainly deposits at the gully outlet and at the left bank of the mainstream, with the deposition shape substantially symmetrical relatively to the central axis (Figure 4) of the tributary gully. Then under the impact of the mainstream backwater, the horizontal expansion of the alluvial fan towards the upstream of the mainstream is restricted. Due to the joint impact of the original landform and the water pressure of the mainstream, the alluvial fan is developed asymmetrically in the view of the plane shape and expands towards the downstream of the mainstream (Figure 5). Moreover, with the increase of incoming debris flow from the tributary gully, the deposition range and thickness are further increased, and the main flow path is further restricted by the debris flow (Figure 6).

Figures 7 and 8 show the debris flow field at different times. Blocked by the deposit of debris flow, the two flow paths in Figure 7 at the initial time (the right tributary directs to the upstream of the mainstream) are gradually converted to a single flow path close to the left bank of the

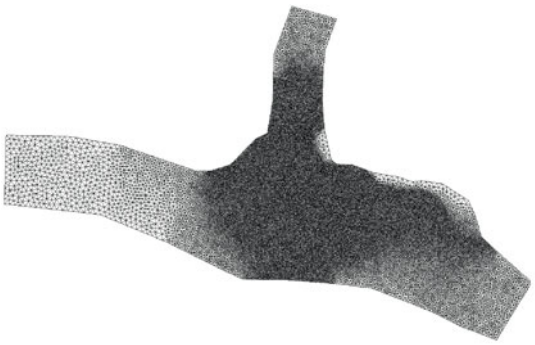

Figure 3 Adaptive refined grid.

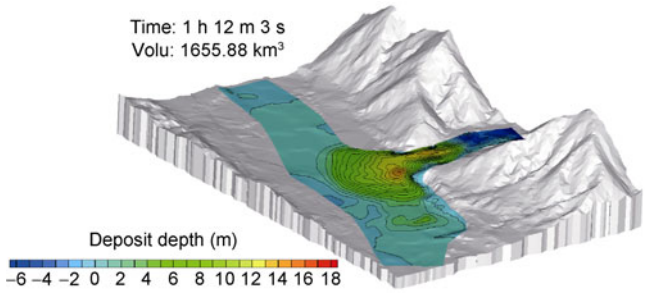

Figure 4 Isogram of deposition thickness in the deposition area (1 h and 12 min).

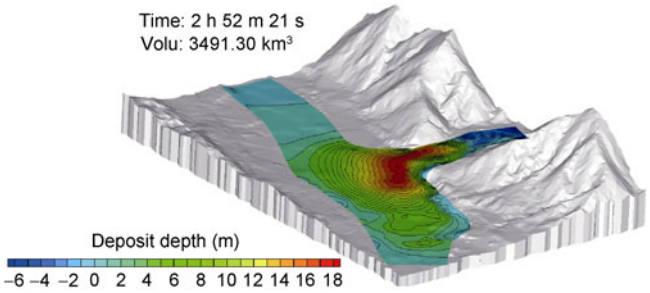

Figure 5 Isogram of deposition thickness in the deposition area (2 h and 52 min).

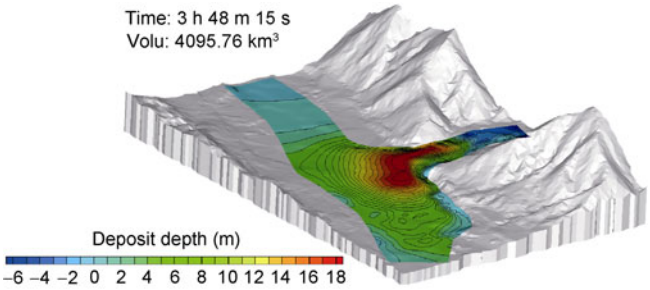

Figure 6 Isogram of deposition thickness in the deposition area (3 h and 40 min).

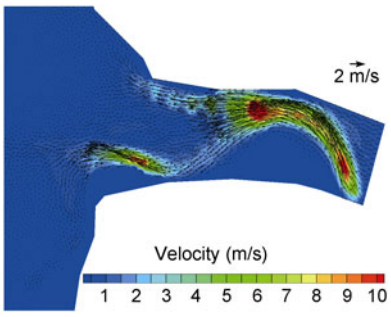

Figure 7 Debris flow velocity isogram in case of 2.17 million cubic meters deposit.

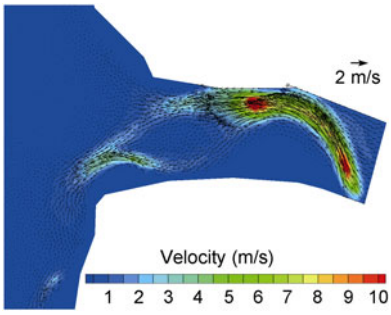

Figure 8 Debris flow velocity isogram in case of 4.53 million cubic meters deposit.

tributary gully and towards the downstream of the mainstream as shown in Figure 8.

The mainstream water depth isograms before and after the debris flow deposition (Figures 9 and 10) show that the mainstream flow path conspicuously shifts to the right, restricted by the debris flow deposit. Under natural conditions, the mainstream flow path bends and runs through Wenjiagou Gully Mouth. When restricted by the landform at the right bank, it runs along the front edge of the original alluvial fan of Wenjiagou and towards the Wenjiagou side at the left bank. However, after the debris flow, as the elevation of the Wenjiagou Gully Mouth increases, the mainstream flow is forced to run along the highland at the right bank of the alluvial fan front edge (Qipan Village) straightly and smoothly and the river channel shape is changed greatly.

The river channel water depth map after the debris flow (Figure 10) shows significant increase of the water depth at the upstream of the deposit, which indicates the conspicuous water raising effect at the upstream of the deposit due to silt-up of the riverbed and decrease of the effective flow width of the river channel at Wenjiagou Gully Mouth section. The decrease of the water depth at the lower edge of the deposit is caused by the silt-up of the bed surface (impacted by water blocking at the Old Qingping Bridge at the downstream, in water raising state).

The mainstream flow field both before and after debris flow deposition are shown in Figures 11 and 12. It is shown that the natural mainstream flow bends, runs rapidly at the gully mouth and the upstream reach and doesn't run through the right bank. The flow path changes greatly after the debris flow deposition, i.e., the main stream shifts to the right and the water flow velocity at the gully mouth reach increases greatly. At the upstream of the deposit, impacted by elevation of the landform, the water flow velocity reduces largely, which provides conditions for sedimentation in the mainstream, while at the lower edge reach of the deposit, the water flow diffuses and the shoreward rapid water flow will erode the river bank. It can be seen that due to the debris flow deposition, not only the river channel water level is elevated, but also the riverbank will be subject to lateral erosion, which would adversely impact on the flood control of the river channel and the stability of the river regime.

The sediment transport capacity of the mainstream will also impact the deposition of the debris flow. In this case, the deposit of the debris flow narrows the effective flow width of the mainstream and thus increases the sediment transport capacity of the downstream of the mainstream, and partial deposits are eroded downstream by the mainstream to reduce the deposition speed of the debris flow in the deposition area. The debris flow deposition hydrograph in Figure 13 shows gradual decrease of deposition speed in spite of gradual increase of total deposition amount. Figure 14 shows the landform elevation isogram when the debris flow deposition amount is 4.50 million cubic meters.

Due to lack of field real-time observation data, the simulated 5 h (Wenjiagou debris flow lasted for about 5 h) debris flow deposition thickness (Figure 15) and field measured

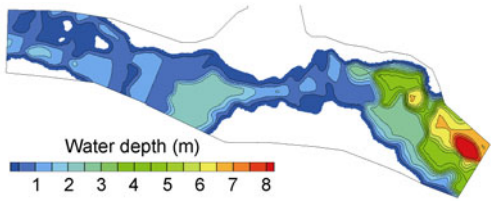

Figure 9 Mainstream water depth map before debris flow deposition.

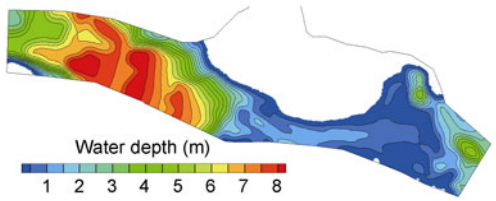

Figure 10 Mainstream water depth map after debris flow deposition.

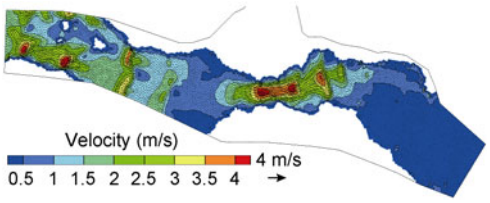

Figure 11 Mainstream flow field map before debris flow deposition.

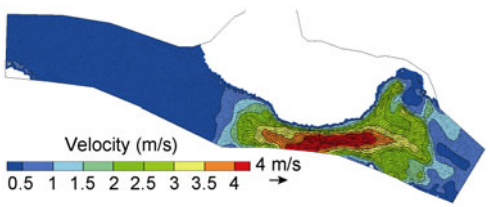

Figure 12 Mainstream flow field map after debris flow deposition.

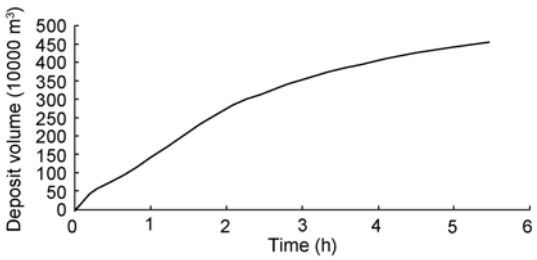

Figure 13 Hydrograph of debris flow deposition.

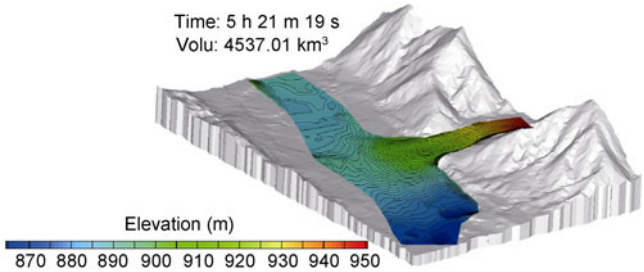

Figure 14 Landform elevation isogram when the deposition amount is 4.50 million cubic meters.

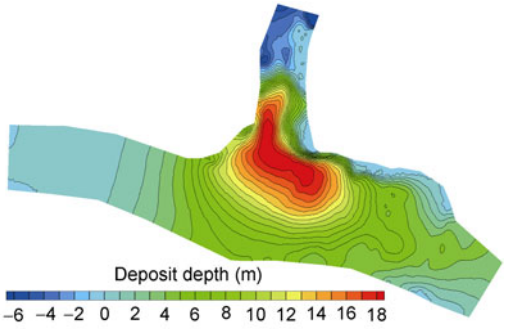

Figure 15 Isogram of deposition thickness in the simulated deposition area.

3-day deposition landform (Figure 16) were compared with each other. It can be seen that for the largest deposition part and the main deposition area, the calculated deposition thickness and the field-acquired results are substantially similar. For quantitative deposition thickness, the calculated value is a little higher than the field measured value, while for the deposition range, the calculated deposition thicknesses are different from the field measured values at the upstream and downstream of the gully mouth and the opposite bank of the tributary. The reason is that with the completion of the debris flow process, the moisture in the deposit with a high water content in the early stage would be separated out gradually and the deposition thickness would decrease on the whole. At the same time, the subsequent water from the tributary would scour the unconsolidated sediment on the surface of the deposit to form fine- grain slurry with a high sediment concentration to move downstream and cause redistribution of the deposit along

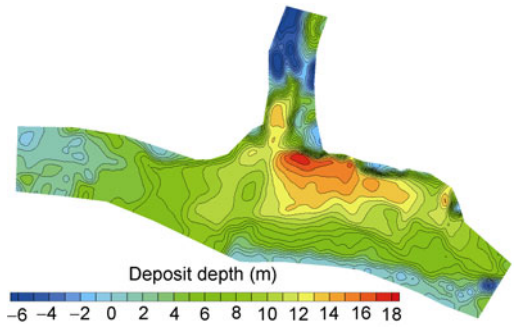

Figure 16 Isogram of deposition thickness in the field measured deposition area.

the tributary flow path. And then the deposit of the debris flow would be subject to a subsequent deformation process at the end of the debris flow process. Besides, some simplifications of the model, modeling of the resistance of debris flow movement and inaccuracy in determination of the initial conditions and boundary conditions will also greatly affect the results of simulation. Therefore, further improvements to the model need to be made in consideration of such aspects.

3.4 Application of model to design of river restoration schemes

The super large-scale torrential flood and debris flow in Aug. 13 caused great losses to the local people, and the reconstruction work after the disaster in May 12, and the river channel deposition caused by debris flow caused the greatest damage and great potential post-disaster safety hazards. In order to reduce the post-disaster risk of debris flow deposition, relevant administrative departments have developed a series of applicable restoration schemes for the river channel, e.g. new excavation of river channel, construction of embankment, stabilization of the mainstream flow path. Figure 17 shows the flow field map for the river channel calculation in the recommended scheme under 20-year flood conditions. However, field survey shows in spite of huge scale of the torrential flood and debris flow, there is still the risk of large-scale debris flow in case of bursting of torrential flood due to 50 million cubic meters solid sources formed by Wenchuan earthquake. So the numerical model is used to predict the change of flow field of newly treated river channel and future flood control capacity in case of occurrence of another debris flow deposition, as useful reference for the design of schemes. Due to space limitations, this paper only gives the debris flow deposition landforms (Figures 18 and 19) when the debris flow deposition amounts in the recommended scheme are 0.5 million cubic meters and 2 million cubic meters (based on the given mainstream and the tributary confluence conditions of the debris flow in Aug. 13). And the river channel flow field in the case of a 20-year flood in the river channel mainstream

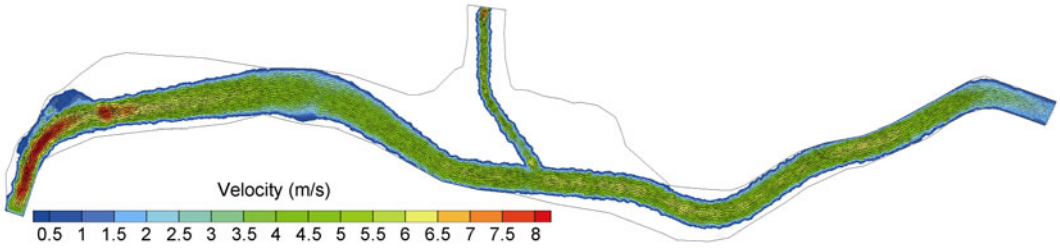

Figure 17 A calculated map of flow field under a 20-year flood after the management of the recommended schemes.

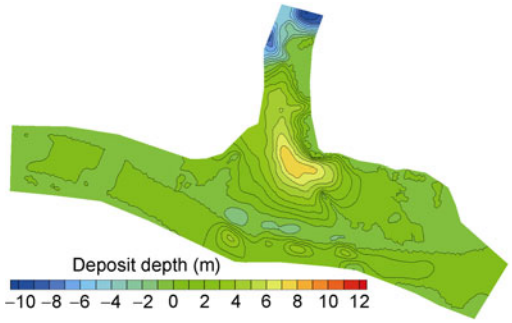

Figure 18 0.5 million cubic meters debris flow deposition map upon treatment as specified in the recommended scheme.

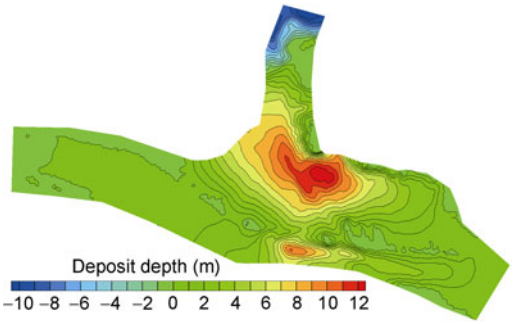

Figure 19 2 million cubic meters debris flow deposition map upon treatment as specified in the recommended scheme.

(Mianyuan River) and the tributary (Wenjiagou) when the debris flow sedimentation amount in the recommended scheme is 2 million cubic meters is shown in Figure 20.

Numerical results of the model show that under the condition of Aug. 13 deposition mode, when the debris flow scale is less than 0.5 million cubic meters, the raised river channel water level is about 1.8 m and new excavation of main channel can still substantially meet the flood passage requirement for 20-year flood. When the debris flow scale is further increased to 2 million cubic meters, the main channel sedimentation thickness opposite to the gully mouth will be above 8 m and the raised water level of the mainstream channel will be approximately 8 m, resulting in great impact on the flood passage capacity of the river channel. These results have been applied to the design of the river restoration schemes.

4 Conclusion and discussion

4.1 Conclusion

In this paper, a mathematical model for confluence of the debris flow was established based on simplification of the interaction mechanism between the debris flow and the mainstream water flow and the model was verified by using the case of recent Qingping Wenjiagou debris flow which converged with Mianyuan River. The conclusions are as follows.

1) Based on the simplified assumption of the model and the effect of the interaction in the confluence zone of the debris flow and the mainstream water flow, a distributed coupling debris flow confluence model is established, by which the debris flow confluence process, the water and sediment movement laws of the mainstream and the tributary during the process can be analyzed. And the distribution of the deposition and its change may also be obtained as well.

2) Finite element CBS algorithm with high stability is

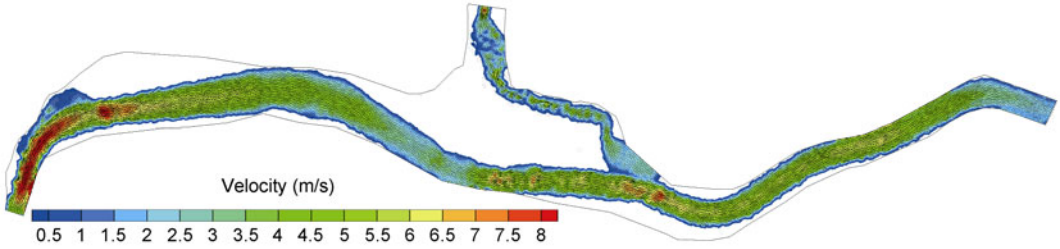

Figure 20 2 million cubic meters debris flow deposited river channel flow field map upon treatment as specified in the recommended scheme.

used for calculation of convection dominated problems, which can increase the stability of the confluence model between the debris flow and the main river water flow on steep slope and expand the application field of CBS algorithm.

3) The recent Qingping Wenjiagou debris flow confluence case is simulated and field-acquired deposited landform is used for verification of the model. The results show that the deposition range and thickness distribution are consistent with the measured results qualitatively. With the consideration of the subsequent impact of deformation of the measured landform, the results calculated with the model are relatively satisfactory.

4.2 Problems and discussion

The debris flow confluence involves the interaction between the Newtonian fluid and the non-Newtonian fluid, and has a complex physical mechanism. In this paper, simplified assumptions were made and a numerical confluence model was established, which obtained good simulated results qualitatively but is still with large errors quantitatively. In order to increase the accuracy and applicability of the results calculated with the model, the following improvements need to be made.

1) Optimization of physical mechanism. The model in this paper is established based on the generalized assumption. The interaction between the debris flow and the water flow, with the development of the debris flow confluence theory, may be improved to optimize the model theoretically.

2) Improvement of confluence conditions. One of the main problems of the model is accurate determination of the debris flow confluence conditions. In order to increase the calculation accuracy of the model, more accurate debris flow confluence conditions can be provided with reference to the study results from analysis of runoff and sediment yields of water basins without data or records.

3) Finite element CBS algorithm is a calculation method based on physical process, so the calculation has a relatively high stability but also a great amount of calculation. CBS and other algorithms may be integrated in the future for further improvement of the model.

This work was supported by the National Basic Research Program of China ("973" Project) (Grant No. 2011CB409903) and the National Natural Science Foundation of China (Grant No. 50739002).

1 Zhu P Y, Cheng Z L, You Y. Discussion on causes of river blocking by sediment transport of Peilonggou of Sichuan-Tibet Highway (in Chinese). J Nat Disast, 2002, 9: 80–83
2 Liu X N, Cao S Y, Huang E. A physical modeling case study on sediment disasters of waterpower station in mountain rivers. J Sichuan U (Eng Sci Edit), 2005, 37(suppl): 1–8
3 Chen D M. Mechanism of Confluence Between Debris Flow and the Mainstream. Dissertation of Doctoral Degree. Beijing: China Institute of Water Resources and Hydropower Research, 2000. 5–32
4 Wu J S, Kang Z C, Tian L Q, et al. Observation and Study on Debris Flow of Jiangjiagou of Yunnan Province (in Chinese). Beijing: Science Press, 1990. 26–47
5 Hu C H, Wang Y G, Zhang Y J. Development and prospects of simulating technology for river sedimentation (in Chinese). J China Hydrol, 2006, 26: 36–41
6 Wang G Q. Advances in river sediment research (in Chinese). J Sediment Res, 2007, 2: 64–81
7 Li T J, Wang G Q, Xue H. Soil erosion and sediment transport in the gullied Loess Plateau: Scale effects and their mechanisms. Sci China Tech Sci, 2009, 52: 1283–1292
8 Fu X D, Jiang L W, Wu B S, et al. Sediment delivery ratio and its uncertainties on flood event scale: Quantification for the Lower Yellow River. Sci China Tech Sci, 2010, 53: 854–862
9 Wang G Q, Ni J R. Basic equations of debris flow dynamics (in Chinese). Chin Sci Bull, 1994, 39: 1700–1704
10 Hübl J, Steinwendtner H. Two-dimensional simulation of two viscous debris flows in Austria. Phys Chem Earth, 2001, 26: 639–644
11 Iovine G, D'Ambrosio D, Di Gregorio S. Applying genetic algorithms for calibrating a hexagonal cellular automata model for the simulation of debris flows characterised by strong inertial effects. Geomorphology, 2005, 64: 287–303
12 Diego B, James T J, Michele L. Debris flows: Recent advances in experiments and modeling. Adv Geophys, 2010, 52: 103–138
13 Lan Z X, Zhou C H, Wang X B. A literature review on debris flow constitutive model and its dynamic simulation (in Chinese). J Eng Geol, 2007, 15: 314–321
14 Wang G Q, Shao S D, Fei X J. Particle model for simulating flow over large area. J Hydraul Eng, ASCE, 1998, 5: 554–557
15 Hayashi T D, Ichibashi T. Study on bed load transport of sediment mixture. Proc. 24th Jap. Con., 1980
16 Hu J. Mechanism of Confluence Between Debris Flow and Mainstream and Numerical Simulation of Debris Flow Movement. Dissertation of Masteral Degree. Beijing: China Institute of Water Resources and Hydropower Research, 2002. 58–70
17 Zienkiewicz O C, Codina R. A general algorithm for compressible and incompressible flow, Part 1. The split characteristic based scheme. Int J Num Meth Fluids, 1995, 20: 869–885
18 Zienkiewicz O C, Taylor R L. The Finite Element Method 6th ed. Volume 3: Fluid Dynamics. Oxford: Elsevier Ltd., 2006
19 Liu X N. Gravel Bed-load Transport and its Modelling. Dissertation of Doctoral Degree. Chengdu: Sichuan University, 2004. 42–50
20 Zienkiewicz O C, Taylor R L. The Finite Element Method 6th ed. Volume 1: The Basis. Oxford: Elsevier Ltd., 2006